Reduction of Computational Complexity in the Butterfly Search Technique

Sheikh Kaisar Alam and Kevin J. Parker,* *Fellow, IEEE*

Abstract— **In the butterfly search technique, echoes from repeated firings of a transducer are resampled along a set of predetermined trajectories of constant velocities, called "butterfly lines," because of their intersection and crossing at a reference range. The slope of the trajectory on which the sampled signals satisfy a predetermined criterion appropriate for the type of signal in question, provides an estimate of the velocity of the target. The search for this trajectory is called "butterfly search," which can be carried out efficiently in a parallel processing scheme. The estimator can be based on the radio frequecy (RF) A-lines, the envelopes, or the quadrature components. The butterfly search on quadrature components has shown outstanding noise immunity, even with relatively few successive scan lines, and was found to outperform all the common time domain and Doppler techniques in simulations and experiments with strong noise. It can be simply implemented using elementary digital signal processing hardware. However, it is possible to further improve upon its computational complexity to make the technique even simpler to implement, without any complex multipliers in the parallel channels. In this paper, we present some modifications that significantly reduce the computational complexity of butterfly search on quadrature components.**

I. Introduction

REAL-TIME ultrasonic blood flow velocity measurement and color flow imaging are very important in disease diagnosis. Much of the previous work in this field can be divided into two major categories: 1) methods that make use of the change of phase in the quadrature components of successive radio frequency (RF) A-lines ("Doppler" techniques: [1]–[3]), and 2) methods that make use of the time shift in the envelope or RF reflection using correlation methods ("time domain" techniques: [4]–[7]) due to repeated firings of the transducer. The majority of commercial scanners use a narrowband technique for color flow imaging that is based on an autocorrelation algorithm [3]. Please see [8]–[10] for a review of "Doppler" frequency estimation and [11] for a review of time domain techniques. Mo *et al.* [12] presented a detailed discussion on various maximum frequency estimators for Doppler ultrasound. However, all of these methods have inherent tradeoffs. A relatively long tone burst is needed to accurately measure the velocity with the Doppler techniques. That decreases the flow imaging resolution. In the time domain techniques, correlation windows must be fixed, and extensive calculations over many echo pairs are required. More recently, an important matched filter approach to a wideband maximum likelihood estimator of velocity was developed by Ferrara and Algazi [13], [14]. We independently developed a technique called the butterfly search [15] that is based on a deterministic tracking of a moving scatterer's echo in two-dimensional (2-D) (slow time, fast time) space. When applied on quadrature components, it can outperform the conventional techniques in extremely unfavorable conditions. It can be realized in hardware using elementary digital operations. However, it is possible to greatly improve upon its computational complexity to make the technique even more attractive for real-time, hardware implementation. In this paper, we discuss some modifications that will significantly reduce the computational complexity of the butterfly search on quadrature components. The effect on hardware multiplication is explored. The proposed computational complexity reduction can be achieved in two ways. In one case, the multiplication of the butterfly sampled complex envelope by the complex exponential in the numerator of (5) in this paper is replaced by multiplying the complex envelope by an RF complex exponential before the butterfly sampling step. In the other case, the quadrature demodulation and the premultiplication step is shown to be equivalent to passing the RF echo through a Hilbert transform step. This paper is organized as follows. First we review the butterfly search on quadrature components that was introduced in the concept paper [15]. We first show the simplifications for the point target case, and then we take a multiple scatterer case where all the scatterers are moving at the same velocity. Then we demonstrate typical savings in computation. In addition, we provide performance results of the reduced computation approaches using simulation, phantom and flow phantom data.

Manuscript received March 14, 1995; revised February 26, 1996. This work was supported in part by the Department of Electrical Engineering and the NSF/NYS Center for Electronic Imaging System, University of Rochester, Rochester, NY. *Asterisk indicates corresponding author.*

S. K. Alam is with the Department of Radiology, Ultrasonics Laboratory, University of Texas Medical School, Houston, TX 77030 USA.

*K. J. Parker is with the Department of Electrical Engineering and Center for Biomedical Ultrasound, University of Rochester, Rochester, NY 14627 USA (e-mail: parker@ee.rochester.edu).

Publisher Item Identifier S 0018-9294(96)04834-3.

II. Reduction of Computational Complexity

A. Point Spread Target

1) Review of Butterfly Search: In the butterfly search technique, a search is performed along trajectories which describe lines of constant velocity in 2-D (slow time—transducer firing index, fast time—range) space. In Fig. 1, a quadrature component of the RF echoes (shown Gaussian) from a single moving scatterer is shown along with the search trajectories. As the scatterer moves, the echoes shift in time. The complex envelope, sampled along the trajectory of correct constant velocity (the solid line in Fig. 1), would consist of single

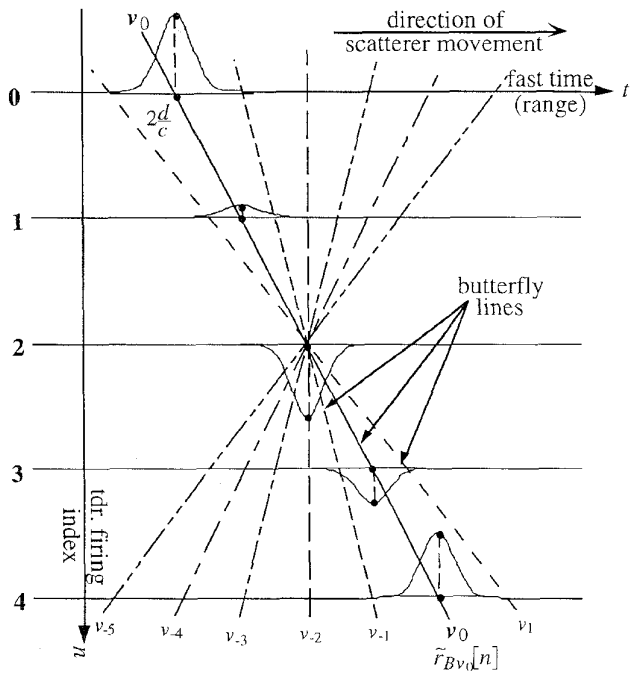

Fig. 1. Illustration of the butterfly search applied on the quadrature components (one shown). Only the solid line would sample a constant amplitude sinusoidal function $\tilde{r}_{Bv_0}[n]$.

frequency sinusoids. Consider a reference sample point at the middle of the RF A-lines. Then sample the signal at different delays between successive RF A-lines (or on different butterfly lines). The butterfly line on which the sampled complex envelope has the expected frequency would be chosen to estimate the scatterer velocity.

The quantization effect in the velocity estimates from the finite number of butterfly lines used in the estimation can be minimized by taking a large number of lines. Since taking large number of lines increase the computational complexity, a compromise between quantization error and computational complexity has to be made. On the other hand, a computationally more attractive approach would be to use a smaller number of butterfly lines in conjunction with interpolation to estimate the velocity when it falls between two quantized velocities.

For the purpose of illustration, let us consider an object moving toward the transducer (for simplicity, a point target is being used). As the object advances, the phase of the echo from the target changes corresponding to the amount the target has moved between successive transducer firings. If its velocity, v_0, is constant, then the waveform for the nth echo (or the nth RF A-line) would have the form

$$s(n,t) = A\cos\left\{\omega_0\left[t - 2\frac{d}{c} + 2n\frac{v_0}{c}T\right]\right\} \cdot r\left\{t - 2\frac{d}{c} + 2n\frac{v_0}{c}T\right\}; \quad n = 0,1,2,\cdots,N \tag{1}$$

where A is the signal amplitude, n is the slow-time index, T is the pulse repetition period, d is the initial distance of the object from the transducer, ω_0 is the angular center frequency, $r(t)$ is the envelope of the transmitted pulse (can be Gaussian, maximizing at $t = 0$), and the factor of two in the expression comes from the round trip travel of the wave. The time-axis origin is reset each time transducer fires. Other system effects are neglected.

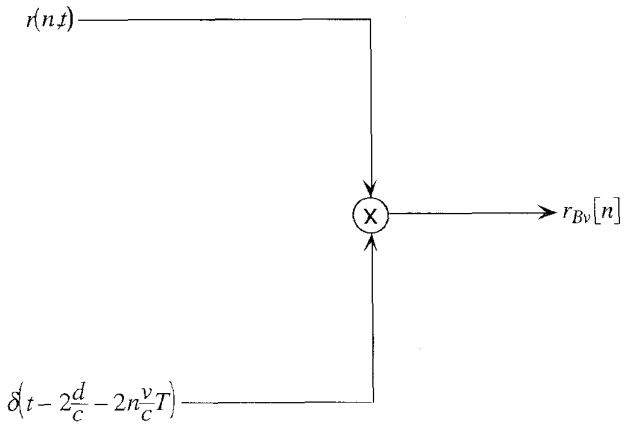

Fig. 2. Butterfly sampler.

The complex envelope for $s(n,t)$ is

$$\tilde{r}(n,t) = \frac{A}{2}\exp j\left[2\omega_0\left(\frac{d}{c} - n\frac{v_0}{c}T\right)\right] r\left\{t - 2\frac{d}{c} + 2n\frac{v_0}{c}T\right\} = \tilde{A}\exp -j\left[2\omega_0 n\frac{v_0}{c}T\right] r\left\{t - 2\frac{d}{c} + 2n\frac{v_0}{c}T\right\}, \text{ where}$$

$$\tilde{A} = \frac{A}{2}\exp j\left[2\omega_0\frac{d}{c}\right]. \tag{2}$$

We define $\tilde{r}_{Bv}[n]$ to denote the resampling of the complex envelope along the butterfly line for velocity v, to estimate the velocity at depth d

$$\tilde{r}_{Bv}[n] = \tilde{r}(n,t)\delta\left(t - 2\frac{d}{c} + 2n\frac{v}{c}T\right). \tag{3}$$

Here we assume that the impulse train of the sample function is implicitly followed by a conversion to a discrete time sequence (a continuous-to-discrete (C/D) conversion in the conventional sense) [16].

Then on the correct butterfly line

$$t - 2(d/c) + 2n(v_0/c)T = 0$$

$$\tilde{r}_{Bv_0}[n] = \tilde{A}\exp -j\left[2\omega_0 n\frac{v_0}{c}T\right] r(0). \tag{4}$$

Thus, it is a single frequency and constant amplitude [actually maximum amplitude since $r(t)$ maximizes at $t = 0$] function only on the correct line. Discrete samples rather than continuous time waveform would be used in actual implementations, and thus, a point on the butterfly line may lie between two successive samples. Linear interpolation between successive samples can be used in such cases to estimate the signal value on the butterfly line.

The velocity is estimated using (5) and (8).

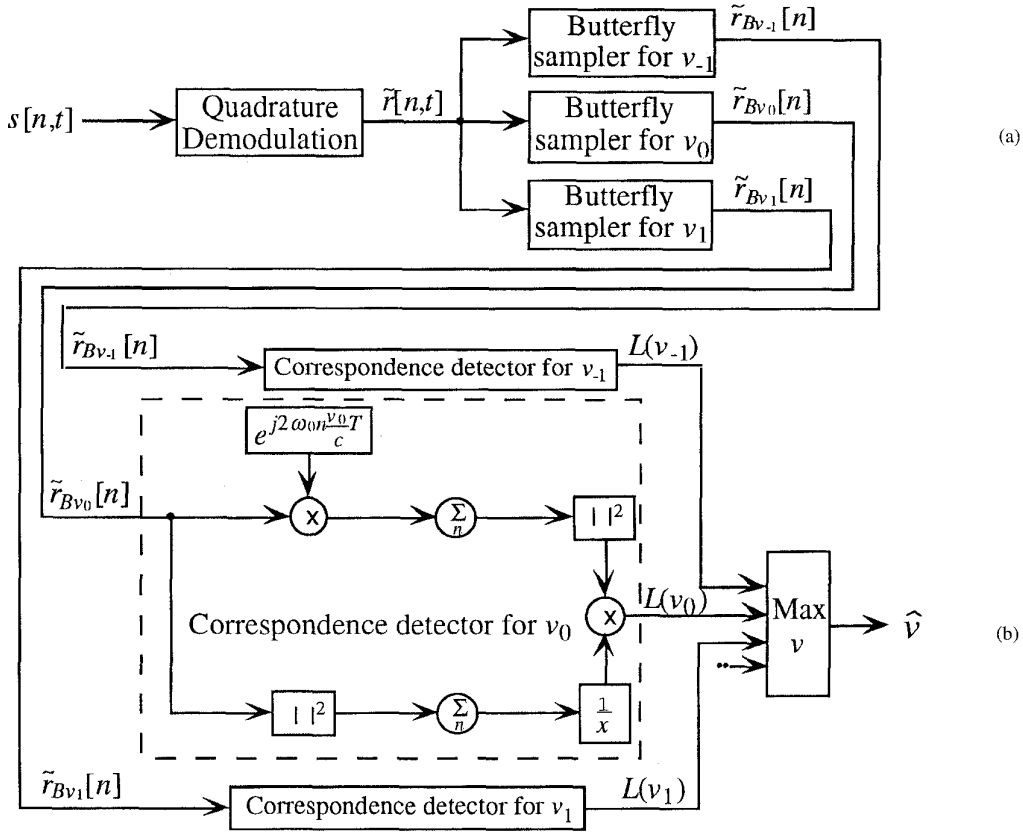

Fig. 3. Schematic hardware diagram for quadrature butterfly search; (a) butterfly sampling of complex envelope, (b) processing $\tilde{r}_{Bv}[n]$ to extract $\hat{v}$.

For the blood velocity estimation using Butterfly search on quadrature components, we evaluate [15]

$$L(v) = \frac{\left|\sum_n \tilde{r}_{Bv}[n] e^{j2\omega_0 n(v/c)T}\right|^2}{\sum_n |\tilde{r}_{Bv}[n]|^2} = \frac{A(v)}{B(v)} \tag{5}$$

where, $\tilde{r}_{Bv}[n]$ is the butterfly sampled signal in (3)

$$A(v) = \left|\sum_n \tilde{r}_{Bv}[n] e^{j2\omega_0 n(v/c)T}\right|^2 \tag{6}$$

and

$$B(v) = \sum_n |\tilde{r}_{Bv}[n]|^2. \tag{7}$$

By Schwarz inequality, $L(v)$ maximizes when $\tilde{r}_{Bv}[n]$ closely corresponds to the complex conjugate of the expected return $e^{-j2\omega_0 n(v/c)T}$ from a moving scatterer on the butterfly line.

We determine the velocity by finding the maximum of $L(v)$

$$\hat{v} = \max_v \{L(v)\}. \tag{8}$$

The mean velocity can be evaluated by finding the following weighted mean

$$\overline{v} = \frac{\sum_i v_i L(v_i)}{\sum_i L(v_i)}. \tag{9}$$

The schematic hardware diagram for the butterfly search on complex envelope is shown in Fig. 3. Here $\tilde{r}_{Bv}[n]$ are sampled following the quadrature demodulation step at the butterfly sampler banks (a typical butterfly sampler for any velocity v is shown in the schematic diagram Fig. 2). The output from each sampler then goes through a "correspondence detector" which executes the following steps: multiplication by a complex exponential, summation (over index n), followed by magnitude square and a normalization by a quantity derived by magnitude square followed by summation (over index n). This would produce the $L(v)$ values, which are input into a maximum detector. The velocity corresponding to the maximum $L(v)$ is the velocity estimate. Clearly, generation of the complex exponential and multiplying it by the butterfly sampled complex envelope heavily contributes to the computation. Since this complex exponential multiplication takes place within each parallel butterfly channel, there is a significant cost associated with these multiplications. Simplification of the implementation follows.

2) Premultiplication by Complex Exponential: The simplification in $L(v)$ can be done by rewriting both its numerator and the denominator.

From (6)

$$\begin{aligned}A(v) &= \left|\sum_n \tilde{r}_{Bv}[n]e^{j2\omega_0 n(v/c)T}\right|^2 \\ &= \left|\sum_n \tilde{r}(n,t)\delta\left(t-2\frac{d}{c}+2n\frac{v}{c}T\right)e^{j2\omega_0 n(v/c)T}\right|^2 \\ &= \left|\sum_n \tilde{r}(n,t)\delta\left(t-2\frac{d}{c}+2n\frac{v}{c}T\right)e^{j2\omega_0 n(v/c)T}\right|^2 \\ &\quad \cdot |e^{-j2\omega_0(d/c)}|^2, \quad \text{since } |e^{-j2\omega_0(d/c)}| = 1 \\ &= \left|\sum_n \tilde{r}(n,t)\delta\left(t-2\frac{d}{c}+2n\frac{v}{c}T\right)\right. \\ &\quad \left.\cdot\, e^{-j2\omega_0((d/c)-n(v/c)T)}\right|^2 \\ &= \left|\sum_n [\tilde{r}(n,t)e^{-j\omega_0 t}]\delta\left(t-2\frac{d}{c}+2n\frac{v}{c}T\right)\right|^2 \\ &= \left|\sum_n \tilde{r}p_{Bv}[n]\right|^2 \end{aligned} \tag{10}$$

where

$$\tilde{r}p_{Bv}[n] = [\tilde{r}(n,t)e^{-j\omega_0 t}]\delta\left(t-2\frac{d}{c}+2n\frac{v}{c}T\right). \tag{11}$$

And, from (7)

$$\begin{aligned}B(v) &= \sum_n |\tilde{r}_{Bv}[n]|^2 \\ &= \sum_n \left|\tilde{r}(n,t)\delta\left(t-2\frac{d}{c}+2n\frac{v}{c}T\right)\right|^2 \\ &= \sum_n \left|[\tilde{r}(n,t)e^{-j\omega_0 t}]\delta\left(t-2\frac{d}{c}+2n\frac{v}{c}T\right)\right|^2, \text{ since} \\ &\quad |e^{-j\omega_0 t}| = 1 \\ &= \sum_n |\tilde{r}p_{Bv}[n]|^2. \end{aligned} \tag{12}$$

Thus, the numerator of $L(v)$ can be evaluated by multiplying the complex envelope with $e^{-j\omega_0 t}$ prior to butterfly sampling and summing the butterfly sampled signals, instead of the original technique where samples on each butterfly line had to be multiplied by a unique complex exponential before the summation in the numerator. This can add up to substantial savings in complex multiplications.

Thus, (5) can be rewritten as the following:

$$L(v) = \frac{A(v)}{B(v)} = \frac{\left|\sum_n \tilde{r}p_{Bv}[n]\right|^2}{\sum_n |\tilde{r}p_{Bv}[n]|^2} \tag{13}$$

where $\tilde{r}p_{Bv}[n]$ is given in (11).

Thus, the correspondence detector is greatly simplified in the premultiplied butterfly search method. In this new approach, the quadrature signals are multiplied by an RF complex exponential, which are then butterfly sampled. Outputs from the butterfly samplers $\tilde{r}p_{Bv}[n]$ are fed to the simplified correspondence detectors. The velocity corresponding to the largest correspondence, detected by a maxima detector, is the estimated velocity. This schematic hardware is shown in Fig. 4. Here, we were able to do away with the complex exponential generation and multiplication step within the parallel correspondence detector stages.

3) Complex RF: From (1), the nth reflection from a point target moving away from the transducer at a velocity v_0 would have the form

$$\begin{aligned}s(n,t) &= A\cos\left\{\omega_0\left[t-2\frac{d}{c}+2n\frac{v_0}{c}T\right]\right\} \\ &\quad \cdot r\left\{t-2\frac{d}{c}+2n\frac{v_0}{c}T\right\} \quad n=0,1,2,\cdots,N \\ &= \frac{A}{2}\left[\exp j\left\{\omega_0\left(t-2\frac{d}{c}+2n\frac{v_0}{c}T\right)\right\}\right. \\ &\quad \left.+\exp -j\left\{\omega_0\left(t-2\frac{d}{c}+2n\frac{v_0}{c}T\right)\right\}\right] \\ &\quad \cdot r\left\{t-2\frac{d}{c}+2n\frac{v_0}{c}T\right\}. \end{aligned} \tag{14}$$

If we premultiply the complex envelope with the complex exponential, we get

$$\begin{aligned}\tilde{r}(n,t)e^{-j\omega_0 t} &= \frac{A}{2}\exp j\left\{2\omega_0\left(\frac{d}{c}-n\frac{v_0}{c}T\right)\right\} \\ &\quad \cdot r\left\{t-2\frac{d}{c}+2n\frac{v_0}{c}T\right\} \\ &\quad \cdot e^{-j\omega_0 t} \\ &= \frac{A}{2}\exp -j\left\{\omega_0\left(t-2\frac{d}{c}+2n\frac{v_0}{c}T\right)\right\} \\ &\quad \cdot r\left\{t-2\frac{d}{c}+2n\frac{v_0}{c}T\right\}. \end{aligned} \tag{15}$$

By comparing (14) and (15) we see that (15) can be obtained from the RF signal by just zeroing the positive frequency part in (14).

Then

$$L(v) = \frac{\left|\sum_n \tilde{r}p_{Bv}[n]\right|^2}{\sum_n |\tilde{r}p_{Bv}[n]|^2} \tag{16}$$

where

$$\begin{aligned}\tilde{r}p_{Bv}[n] &= [\tilde{r}(n,t)e^{-j\omega_0 t}]\delta\left(t-2\frac{d}{c}+2n\frac{v}{c}T\right) \\ &= [s(n,t)^* h(t)]\delta\left(t-2\frac{d}{c}+2n\frac{v}{c}T\right). \end{aligned} \tag{17}$$

$*$ denotes convolution

$$H(f) = \mathcal{F}\{h(t)\} = \begin{Bmatrix}1, & f<0\\ 0, & f\geq 0\end{Bmatrix}. \tag{18}$$

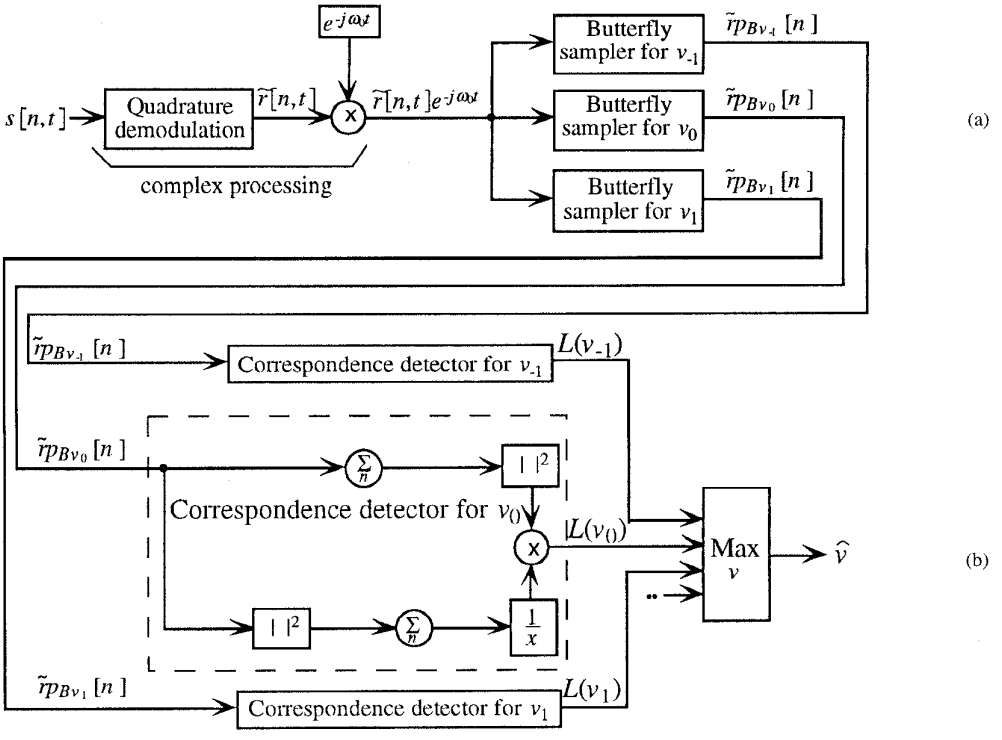

Fig. 4. Schematic hardware diagram for premultiplied butterfly search; (a) sampling premultiplied complex envelope and (b) processing of $\tilde{r}p_{Bv}[n]$ to extract $\hat{v}$.

This can further reduce the computational complexity, because this does away with complex envelope computation. Schematic hardware for the complex RF butterfly search is shown in Fig. 5, which is almost identical to the hardware shown in Fig. 4. The only difference is that the complex processing step involving quadrature demodulation followed by multiplication with complex exponential is substituted by an operator based on Hilbert transform. Furthermore, using look up tables for squaring and inverse function would remove all complex multiplication in the correspondence detection step and thus, reduce the computational complexity even more.

B. Multiple Targets

Now we verify that the simplifications methods derived in the previous section would be valid in presence of more than one scatterer.

If there are more than one scatterers, then the reflected echoes would be

$$s(n,t) = \sum_i a_i \cos\left\{\omega_0\left[t - 2\frac{d_i}{c} + 2n\frac{v_0}{c}T\right]\right\} \cdot r\left\{t - 2\frac{d_i}{c} + 2n\frac{v_0}{c}T\right\} \quad n = 0,1,2,\cdots \tag{19}$$

where a_i is the reflection amplitude associated with the ith scatterer (which depends on various factors such as distance from transducer, scattering cross section, etc.), d_i is the distance of the ith scatterer from the transducer at the first firing ($n = 0$). The assumption is that all the scatterers move at the same velocity v_0, and no system effect is accounted for in this model.

Then the complex envelope is

$$\tilde{r}(n,t) = \sum_i \frac{a_i}{2} \exp j\left[2\omega_0\left(\frac{d_i}{c} - n\frac{v_0}{c}T\right)\right\} \cdot r\left\{t - 2\frac{d_i}{c} + 2n\frac{v_0}{c}T\right\} \quad n = 0,1,2,\cdots. \tag{20}$$

For finding velocities at depth d, the butterfly sampled complex envelope is

$$\begin{aligned}\tilde{r}_{Bv}[n] &= \tilde{r}(n,t)\delta\left(t - 2\frac{d}{c} + 2n\frac{v}{c}T\right) \\ &= \sum_i \frac{a_i}{2} \exp j\left[2\omega_0\left(\frac{d_i}{c} - n\frac{v_0}{c}T\right)\right\} \cdot r\left\{2\frac{d}{c} - 2\frac{d_i}{c} + 2n\frac{v_0 - v}{c}T\right\}.\end{aligned} \tag{21}$$

Then, the butterfly samples on the correct line

$$\tilde{r}_{Bv_0}[n] = \sum_i \frac{a_i}{2} \exp j\left[2\omega_0\left(\frac{d_i}{c} - n\frac{v_0}{c}T\right)\right] \cdot r\left\{2\frac{d - d_i}{c}\right\}. \tag{22}$$

Clearly, the scatterers at depth $d = d_i$ will contribute to $\tilde{r}_{Bv_0}[n]$ the most, since $r(\ )$ maximizes at zero. The contributions would fall as $|d - d_i|$ increases. Moreover, on the incorrect butterfly lines, in addition to the incorrect frequency

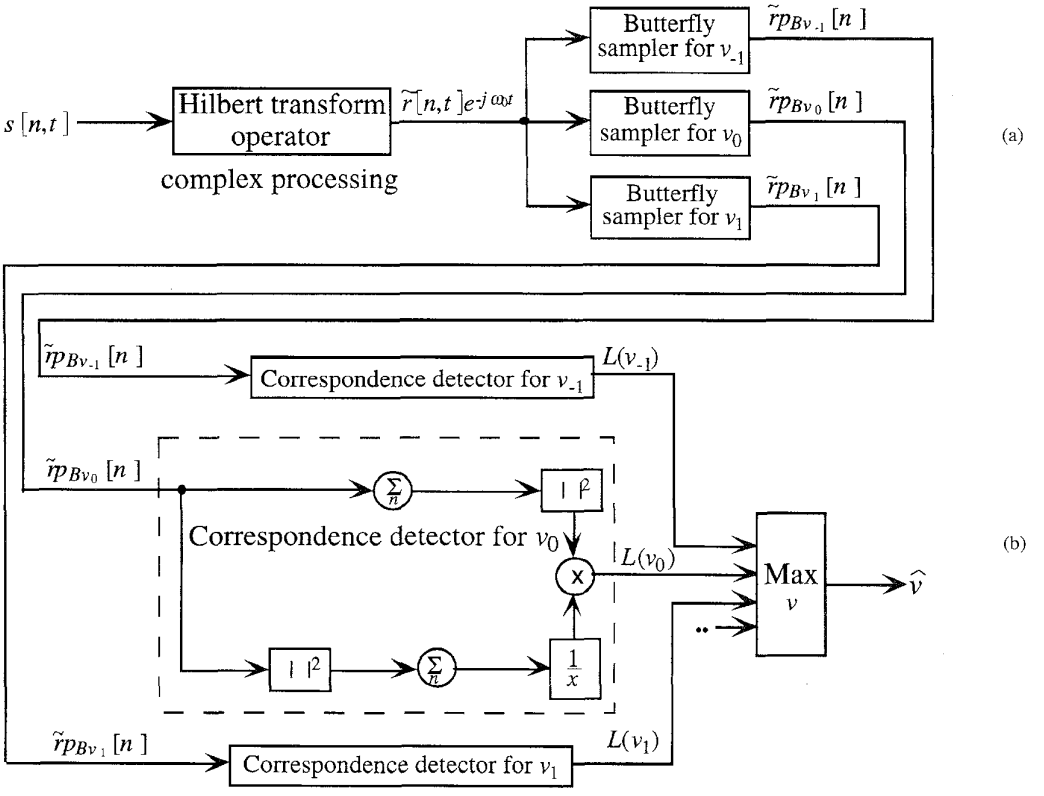

Fig. 5. Schematic hardware diagram for complex RF butterfly search; (a) butterfly sampling complex RF and (b) processing of $\tilde{r}p_{Bv}[n]$ to extract $\hat{v}$.

and variation in amplitude, the neighboring scatterers will also contribute adversely to decrease the value of $L(v)$.

C. Savings in Computation Steps

If we have do an M-point butterfly search estimation, then the number of computation steps is as follows.

The parameters are:

$N =$ number of sample points per scan line,
$M =$ number of RF A-lines used in the estimation,
$L =$ number of butterfly lines per point, and
$K_1 =$ number of estimation points.

The computational complexity is tabulated in Tables I–IV. The cells in light gray contains operations that can be substituted by table lookup or other simple operations.

Just as an illustration, for $N = 1024, M = 3, L = 128$, and $K_1 = 256$, assuming ten bit operations, butterfly search with premultiplication achieves ~43% savings over the original butterfly search on quadrature components. Butterfly search on complex RF, on the other hand, achieves ~45% savings. If the complex RF is obtained by a Hilbert transformer realized with an FIR system [16], the savings would be ~55%. Moreover, the cost of generating the complex exponential in the correspondence detector loop will also be saved. Absolute value and inverse computation can be done using table lookup. In such case, premultiplication butterfly search achieves ~76% savings over the original butterfly search on quadrature components. Complex RF butterfly search, on the other hand, achieves ~80% savings. If complex RF is obtained by a Hilbert transformer, the savings would be ~89%.

D. Using Efficient Search Algorithm

So far, the techniques we talked about used a brute force method for searching the maximum of $L(v)$. However, we can reduce the computation steps even further by using efficient search algorithms, such as hierarchical search [17], especially if the technique has to be implemented in software. Interpolation of $L(v)$ using the discrete maximum and its two nearest neighbors is also an option rather than the brute force method. However, like many computationally simplified approaches, both approaches are inherently suboptimal and it is possible to miss the global maximum in either approach.

E. Practical Considerations

Since blood is a weak scatterer, the signal-to-noise ratio (SNR) of the echo from blood is low. Since additive noise is uncorrelated, spatial averaging of the signal can reduce the detrimental effects of the noise on the velocity estimation. On the other hand, the same operation to reduce noise can be implemented in the frequency domain with an equivalent filter. Because the premultiplied signal and the complex RF signal are more rapidly varying than the complex envelope, filtering of noise have to be adjusted to the frequency content of the signal. Note that the filtering to reduce noise can be done prior to the butterfly sampling step, eliminating the need for that operation in the parallel correspondence detector channels.

TABLE I
BEFORE THE CORRESPONDENCE DETECTOR STEP

Steps		Original Butterfly Search (1)		Butterfly search with Premultiplication (2)		Butterfly search with Complex RF (3)	
		Complex mult.	Complex addition	Complex mult.	Complex addition	Complex mult.	Complex addition
Complex Processing (Complex envelope- 1 & 2, complex RF -3)	Multiply by RF $e^{-j\omega_0 t}$	N		N			
	FFT	$\frac{N}{2} log_2 N$	$N log_2 N$	$\frac{N}{2} log_2 N$	$N log_2 N$	$\frac{N}{2} log_2 N$	$N log_2 N$
	Filter	N		N		N	
	IFFT	$\frac{N}{2} log_2 N$	$N log_2 N$	$\frac{N}{2} log_2 N$	$N log_2 N$	$\frac{N}{2} log_2 N$	$N log_2 N$

TABLE II
NUMERATOR OF $L(v)$, COMPLEX OPERATIONS

Steps		Original Butterfly Search (1)		Butterfly search with Premultiplication (2)		Butterfly search with Complex RF (3)	
		Multiplication	Addition	Multiplication	Addition	Multiplication	Addition
Mult. by compl. exp.	per point	ML		MN			
	for K_1 pt/line	K_1ML		MN§			
Following addition	/point		$L(M-1)$		$L(M-1)$		$L(M-1)$
	K_1 pts.		$K_1L(M-1)$		$K_1L(M-1)$		$K_1L(M-1)$

To further reduce the effect of noise, one can average $L(v)$ over some spatial range (typically less than 1 mm). The velocity corresponding to the maximum of the averaged $L(v)$ will be output as the estimate of velocity for that range.

When points on a butterfly line lie between successive sample points, linear interpolation can be used to estimate the signal value on the butterfly line. However, since the signal is more rapidly varying than the complex envelope in both simplified implementations, this interpolation would also introduce more errors. However, a faster sampling rate would reduce this error.

III. RESULTS

Some comparison results are given in this section. Results given for the one-dimensional (1-D) simulation of three butterfly search techniques discussed in this paper are with three RF A-lines and SNR = 0 dB. The same 1-D simulated data had been used in [15].

For the 1-D simulation, we used a Gaussian RF pulse, with center frequency, $f_0 = 5$ MHz, $f_s = 50 \times 10^6$s, and 10-dB fractional bandwidth of 85.6%. The simulated pulse-repetition frequency (PRF) was 5 kHz. The pulse is shown in Fig. 6.

The pulse was convolved with a line of random scatterers to produce fully developed speckle. Fig. 7 shows the envelope of a scan line, with no additive noise.

Fig. 8 shows $L(v)$ versus v with four RF lines. The true scatterer velocity is -75 cm/s, and there was no additive noise. Original quadrature butterfly, premultiplication butterfly and complex RF butterfly cases are shown. $L(v)$ exhibits a sharp peak at the true velocity of -75 cm/s. There are subsidiary peaks at aliasing interval of $\sim$75 cm/s. There is a slight difference between original quadrature butterfly and the simplified butterfly cases. Both the simplified butterfly search methods produce almost indistinguishable results (only two lines are visible on the graph). The probable reason for the difference between the original and simplified implementations is the interpolation for values when the butterfly lines go between sample points. Quadrature components are slowly varying signals, so interpolation error would be small. But, for premultiplication and complex RF butterfly, the signal

TABLE III
REAL OPERATIONS

Steps		Original Butterfly Search (1)		Butterfly search with Premultiplication (2)		Butterfly search with Complex RF (3)	
Numerator of $L(v)$							
		Multiplication	Addition	Multiplication	Addition	Multiplication	Addition
Abs. value	/point	$2L$	L	$2L$	L	$2L$	L
comp.	$K1$ pts.	$2K_1L$	K_1L	$2K_1L$	K_1L	$2K_1L$	K_1L
Denominator of $L(v)$							
Abs. value	/point	$2ML$	ML	$2ML$	ML	$2ML$	ML
comp.	K_1 pts.	$2K_1ML$	K_1ML	$2K_1ML$	K_1ML	$2K_1ML$	K_1ML
Following Addition	/point		$(M\text{-}1)L$		$(M\text{-}1)L$		$(M\text{-}1)L$
	K_1 pts.		$K_1(M\text{-}1)L$		$K_1(M\text{-}1)L$		$K_1(M\text{-}1)L$
Inverse operations	/point	L		L		L	
	K_1 pts.	K_1L		K_1L		K_1L	
$L(v)$: Numerator/denominator							
Real division	/point	L		L		L	
	$K1$ pts.	K_1L		K_1L		K_1L	

TABLE IV
COMPARISON STEP

Steps		Original Butterfly Search (1)	Butterfly search with Premultiplication (2)	Butterfly search with Complex RF (3)
		Addition	Multiplication	Addition
Abs. value	/point	L -1	L -1	L -1
comp.	K_1 pts.	$K_1(L$ -1)	$K_1(L$ -1)	$K_1(L$ -1)

frequency is substantially higher. Since the frequency contents are different, filtering to reduce noise may also contribute to the difference. The subsidiary peaks are slightly higher for the simplified butterfly search. In general, for both the original and the simplified cases, we have seen the peak to broaden, and the subsidiary peaks to increase as the number of RF A-lines decreases. Addition of noise brings up the base level of the $L(v)$, compared to the peak value $L(v_0)$.

Fig. 9 shows the performance of the three techniques for SNR = 0 dB and three RF lines. Ten bit analog-to-digital (A/D) conversion was emulated. These are very unfavorable conditions to test the robustness of the techniques. The horizontal axis is the actual simulated velocity and the vertical axis is the absolute error in the estimation. The estimation is done only at one range for each simulation. Each simulation used a constant velocity and the range of simulations was -83.75 cm/s to 83.75 cm/s. The butterfly search on quadrature components works well in this extremely unfavorable condition. The butterfly search technique on premultiplied complex envelope and butterfly search technique on complex RF also perform nearly as well and their performances are nearly identical.

The performances of the three techniques are compared in Fig. 10 in an experiment involving progressively moving a phantom. The same data were used in [15] also. In the experiment, the phantom was precisely moved in a computer controlled setup between data acquisitions by a constant distance to simulate velocity. In such an experiment, it is impossible to incorporate any velocity profile. However, it allows to generate precise motion. First part of the experiment was done with no transverse motion and only this set of data was used for the comparison of three butterfly search techniques. Panametrics transducer was used for the scanning. The phantom used was a tissue mimicking material from the ATS labs (Norwalk, CT). The center frequency was 4 MHz and the sampling frequency was 40 MHz. The pulse duration was 1 μs, and the PRF was assumed to be 5 kHz to convert

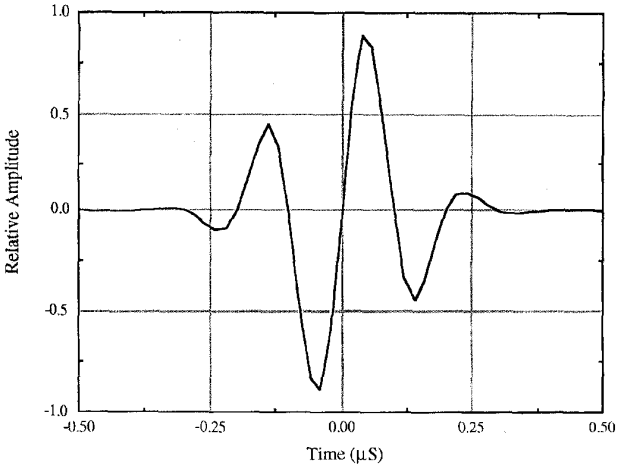

Fig. 6. Pulse fired by the transducer; $\sigma = 1.41$ MHz.

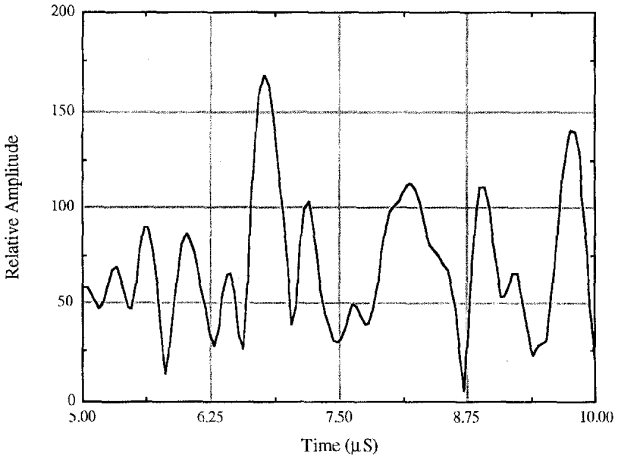

Fig. 7. A line of envelope of echoes from simulation.

time shift to velocity. Data quantization was at ten bits. 2048 sample points were collected for every transducer firing. The number of RF A-lines used in the estimation was three. The estimations were done at a depth of 2.85 cm, where the SNR was approximately 1.65 dB. The overall error is lower for the regular butterfly search on the quadrature components, but, the simplified butterfly techniques have comparable performance.

The geometry of a more involved simulation is shown in Fig. 11. It shows the cross-sectional view of the 3-D scattering volume. A cylindrical vessel, carrying the moving particles, is embedded in the tissue comprised of strong stationary scatterers. The radius of the vessel is unchanged within the image plane and the vessel axis lies on the image plane. The vessel axis is at an angle θ_0 with the beam direction and thus there would be speckle decorrelation because of the lateral movement of the scatterers. Effects of focusing are disregarded. The beam is assumed to be Gaussian in both lateral and azimuthal directions. Thus, the simulation consists of three-dimensional (3-D) random scatterers convolved with a nondiffracting 3-D acoustic pulse. The velocity profile is made to be parabolic ($v = V_{\max}[1-(r/R)^2]$). The ratio of stationary to moving scatterers is 40 dB (i.e., the moving "blood" is hypoechoic). No vessel wall is simulated. The velocity of each scatterer is unchanged through the scanning process.

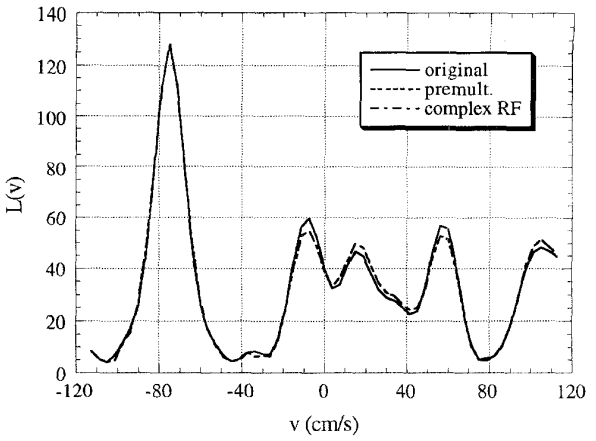

Fig. 8. $L(v)$ versus v for four RF lines for original quadrature butterfly, premultiplication butterfly and complex RF butterfly search. Number of RF lines = 4. Actual velocity is −75 cm/s, no additive noise present. $L(v)$ maximizes at −75 cm/s.

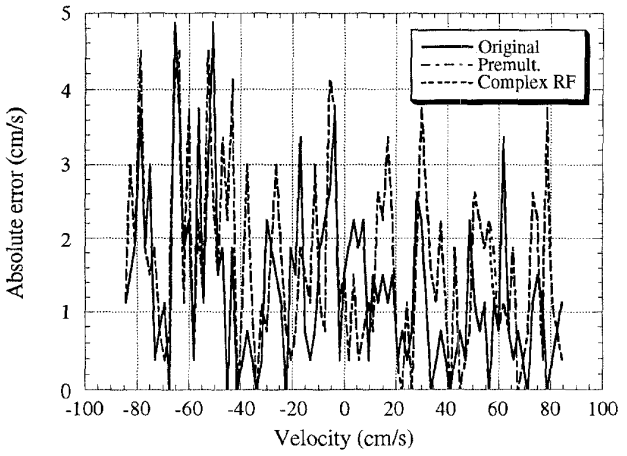

Fig. 9. Comparison of the three butterfly search methods using 1-D simulated data. Number of RF lines = 3, SNR = 0 dB.

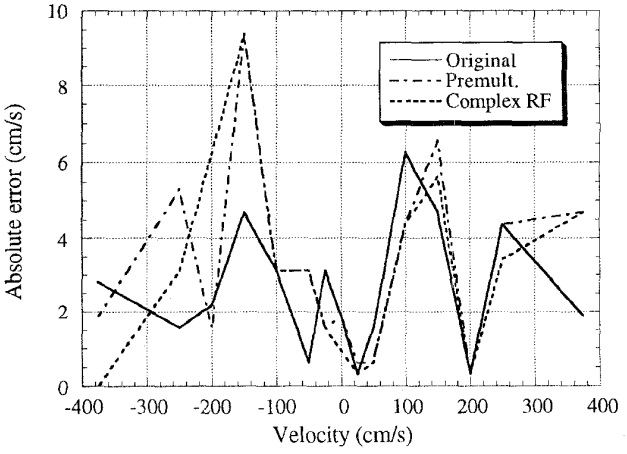

Fig. 10. Comparison of the three butterfly search methods in the phantom experiment. Number of RF lines = 3. Estimated SNR = 1.65 dB.

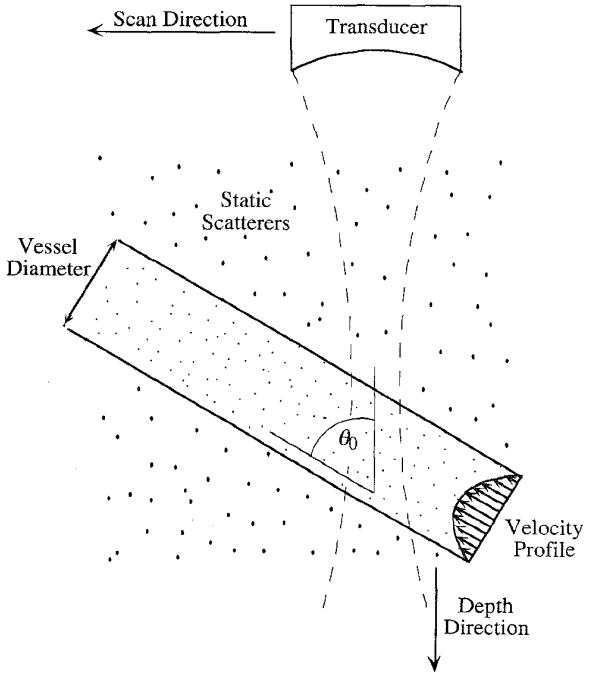

Fig. 11. 3-D scattering volume model. Out of the plane is the transducer azimuthal direction.

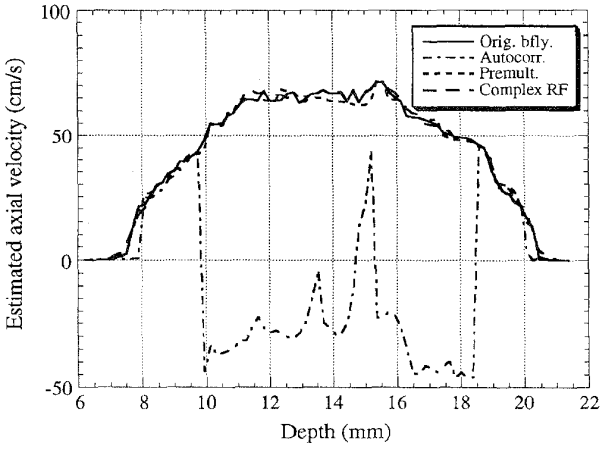

Fig. 12. Comparison of performance of different techniques when applied on the 3-D model. Number of RF lines = 3, SNR = 3 dB.

The performances of different techniques are compared in Fig. 12. Values used were $R = 0.5$ cm, $\theta_0 = 45°$ and $V_{\max} = 100$ cm/s. The vessel boundaries were at 7 mm and 21 mm. The same temporal waveform used in the 1-D simulation was used. The SNR was 3 dB and three RF lines were used in the estimation. All the three butterfly search methods performed quite well. Even at the low-SNR environment, the parabolic profile of the flow is quite nicely reproduced. In comparison, the autocorrelation method shows aliasing. Despite the spatial averaging to reduce the effect of noise, it also shows large error.

Experimental data obtained by Embree [18] has been used for the performance evaluation of different techniques. The data had also been used by Ferrara and Algazi [14] and Vaitkus

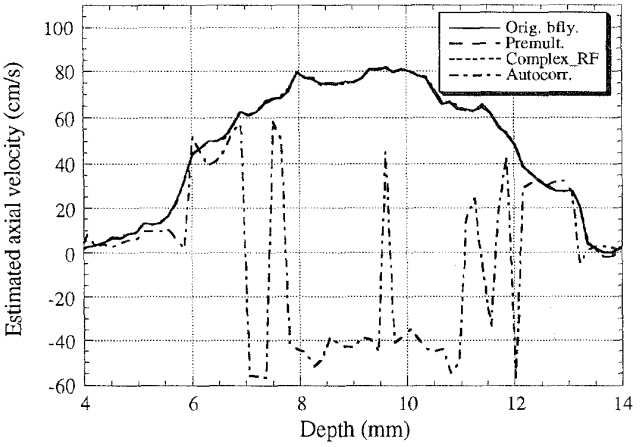

Fig. 13. Comparison of performance of different techniques when applied on flow phantom data. Number of RF lines = 3. SNR = 5 dB.

[19]. The system used Sephadex G-10 particles traveling in a 50% glycerin-water solution through a straight dialysis tube of 7 mm diameter. The angle between the flow and the beam was 45°. The hydrodynamic flow rate was 281 ml/min. Thus, using parabolic flow profile assumption, the peak midstream velocity was 24.3 cm/s. The axial component of this velocity is 17.2 cm/s. The transducer excitation approximated an impulse, the receive bandwidth was approximately 2 MHz and the transducer focal point was located at the midpoint of the vessel. The amplified RF waveform was immediately digitized using 8 bits. A total of 384 A-lines were collected. Each A-line had 1024 samples. The parameters are given below

Transducer center frequency, f_0	5 MHz
RF sampling frequency, f_s	50 MHz
Pulse repetition frequency (PRF)	7812.5 Hz
Range gate delay	54.35 μs
Transducer 1-way 3-dB bandwidth	2.5 MHz
3-dB bandwidth in the focal zone	0.8 mm
Amplifier bandwidth	40 MHz

The estimated flow profiles are shown in Fig. 13. The number of RF lines = 3 and white noise was added to the RF A-lines such that the SNR = 5 dB. We used every fifth RF line for the velocity estimation. Thus, the peak midstream velocity would be 85.9 cm/s. The performance of different techniques is very similar to that in Fig. 12.

IV. Discussions and Conclusions

We have introduced a further improvement to the butterfly search, whereby a premultiplication operator or a Hilbert transform operator is used. A great savings in hardware costs or software multipliers is thereby achieved, as no complex multiplications are then required in the parallel "correspondence detector" stages.

The performance graphs presented provide evidence that simplified butterfly search techniques closely match the accuracy of the original butterfly search technique on quadrature components even with only three RF lines (which would improve the frame rate of color Doppler imaging) in low-SNR environments. However, the results shown are just one

realization from infinitely many possible. A more complete evaluation of competing estimators (simulations and experimental results) over an ensemble can be found in [25].

Recently, the detection of transverse velocity has been investigated by many researchers [20]–[24]. We are currently working on evaluating the natural extension of the butterfly technique to 2-D. Since computational complexity is a limitation in 2-D estimation techniques, the simplified butterfly search methods may prove valuable.

ACKNOWLEDGMENT

The authors would like to thank Dr. X. Chen of the Electrical Engineering Department, University of Rochester for the help in collecting the phantom data. They would like to give special thanks to Dr. P. Embree and Dr. P. Vaitkus for the flow phantom data. They also wish to thank the anonymous reviewers for their insightful comments.

REFERENCES

[1] P. A. Magnin, "Doppler effect: History and theory," *Hewlett Packard J.*, vol. 37, pp. 26–31, 1986.
[2] B. A. J. Angelsen, "Instantaneous frequency, mean frequency, and variance of mean frequency estimators for ultrasonic blood velocity Doppler signals," *IEEE Trans. Biomed Eng.* vol. BME-28, pp. 733–741, 1981.
[3] C. Kasai, K. Namekawa, A. Koyano, and R. Omoto, "Real time two-dimensional blood flow imaging using an autocorrelation technique," *IEEE Trans. Sonics Ultrason.*, vol. SU-32, pp. 458–464, 1985.
[4] O. Bonnefous and P. Pesque, "Time domain formulation of pulse-Doppler ultrasound and blood velocity estimation by cross correlation," *Ultrason. Imag.*, vol. 8, pp. 75–85, 1986.
[5] S. G. Foster, P. M. Embree, W. D. O'Brien, Jr., "Flow velocity profile via time-domain correlation: Error analysis and computer simulation," *IEEE Trans. Ultrason., Ferroelec., Freq. Contr.*, vol. 37, pp. 164–175, 1990.
[6] P. M. Embree and W. D. O'Brien, Jr., "Volumetric blood flow via time-domain correlation: Experimental verification," *IEEE Trans. Ultrason., Ferroelec., Freq. Contr.*, vol. 37, pp. 176–189, 1990.
[7] P. Pesque, "Apparatus for examining a moving object by means of ultrasound echography," U.S. Patent 4 853 904, Aug. 1989.
[8] P. A. Magnin, "A review of Doppler flow mapping techniques," in *Proc. IEEE 1987 Ultrason. Symp.*, 1987, pp. 969–977.
[9] P. J. Vaitkus and R. S. C. Cobbold, "A comparative study and assessment of Doppler ultrasound spectral estimation techniques—I: Estimation methods," *Ultrasound in Med. Biol.*, vol. 14, pp. 661–672, 1988.
[10] P. J. Vaitkus, R. S. C. Cobbold, and K. W. Johnston, "A comparative study and assessment of Doppler ultrasound spectral estimation techniques—II: Methods and results," *Ultrasound in Med. Biol.*, vol. 14, pp. 673–688, 1988.
[11] I. A. Hein and W. D. O'Brien, Jr., "Current time-domain methods for assessing tissue motion by analysis from reflected ultrasound echoes—A review," *IEEE Trans. Ultrason., Ferroelec., Freq. Contr.*, vol. 40, pp. 84–102, 1993.
[12] L. Y. L. Mo, C. M. Y. Louis, and R. S. C. Cobbold, "Comparison of four digital maximum frequency estimators for Doppler ultrasound," *Ultrasound in Med. Biol.*, vol. 14, pp. 355–363, 1988.
[13] K. W. Ferrara and V. R. Algazi, "A new wideband spread target maximum likelihood estimator for blood velocity estimation—I: Theory," *IEEE Trans. Ultrason., Ferroelec., Freq. Contr.*, vol. 38, pp. 1–16, 1991.
[14] ——, "A new wideband spread target maximum likelihood estimator for blood velocity estimation—II: Evaluation of estimators with experimental data," *IEEE Trans. Ultrason., Ferroelec., Freq. Contr.*, vol. 38, pp. 17–26, 1991.
[15] S. K. Alam and K. J. Parker, "The butterfly search technique for estimation of blood velocity," *Ultrasound in Med. Biol.*, vol. 21, pp. 657–670, 1995.
[16] A. V. Oppenheim, A. S. Willsky, with I. T. Young, *Signals and Systems*. Englewood Cliffs, NJ: Prentice-Hall, 1983, pp. 532–533.
[17] M. Bierling, "Displacement Estimation by Hierarchical Blockmatching," in *Proc. SPIE Int. Symp. Visual Commun, Image Processing*, 1988, vol. 1001, pp. 942–951.
[18] P. M. Embree and W. T. Mayo, "Ultrasonic M-mode RF display technique with application to flow visualization," in *Proc. SPIE Int. Symp. Pattern Recog. Acoust. Imag.*, 1987, vol. 768, pp. 70–78.
[19] P. J. Vaitkus, "A new time-domain narrowband velocity estimation technique for Doppler ultrasound flow imaging," Ph.D. dissertation, Dept. Elect. Comput. Eng., Univ. Toronto, 1995.
[20] L. N. Bohs and G. E. Trahey, "A novel method for angle independent ultrasonic imaging of blood flow and tissue motion," *IEEE Trans. Biomed. Eng.*, vol. 38, pp. 280–286, 1991.
[21] V. L. Newhouse, D. Censor, T. Vontz, J. A. Cisneros, and B. B. Goldberg, "Ultrasound Doppler probing of flows transverse with respect to beam axis," *IEEE Trans. Biomed. Eng.*, vol. BME-34, pp. 779–789, 1987.
[22] B. S. Ramamurthy and G. E. Trahey, "Potential and limitations of angle-independent flow detection algorithms using radio-frequency and detected echo signals," *Ultrason. Imag.*, vol. 13, pp. 252–268, 1991.
[23] G. E. Trahey, J. W. Allison, and O. T. von Ramm, "Angle independent ultrasonic detection of blood flow," *IEEE Trans. Biomed. Eng.*, vol. BME-34, pp. 965–967, 1987.
[24] G. E. Trahey, S. M. Hubbard, and O. T. von Ramm, "Angle independent ultrasonic blood flow detection by frame-to-frame correlation of B-mode images," *Ultrason.*, vol. 26, pp. 271–276, 1988.
[25] S. K. Alam, "The butterfly search blood velocity estimation technique for Doppler ultrasound flow imaging," Ph.D. dissertation, Dept. Elect. Eng., Univ. Rochester, 1996.

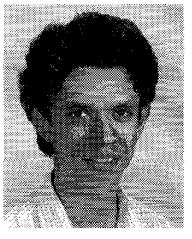

Sheikh Kaisar Alam was born in Rajshahi, Bangladesh. He received the Bachelor of Technology (Hons.) in electronics and electrical communication engineering from the Indian Institute of Technology, Kharagpur, India, in 1986, the MS and Ph.D. degrees in electrical engineering from the University of Rochester, Rochester, NY, in 1991 and 1996, respectively.

He was a Lecturer in the Department of Electrical and Electronic Engineering at the Bangladesh Institute of Technology, Rajshahi, Bangladesh from 1986 to 1989. Since 1995, he has been with the Ultrasonics Laboratory at the University of Texas Medical School at Houston where he has been working on performance characterization and enhancement of elastography. His interests include signal/image processing with applications in medical imaging.

Kevin J. Parker (S'79–M'81–SM'87–F'95) received the Ph.D. degree from Massachusetts Institute of Technology in 1981.

He is currently Professor and Chair of the Electrical Engineering Department at the University of Rochester.

Dr. Parker has received awards from the National Institute of General Medical Sciences (1979), the Lilly Teaching Endowment (1982), the IBM Supercomputing Competition (1989), the World Federation of Ultrasound in Medicine and Biology (1991). He serves as a reviewer and consultant for a number of journals and institutions. He is also a member of the Acoustical Society of America, and the American Institute of Ultrasound in Medicine. He has been named a fellow in the AIUM for his work in medical imaging. In addition, he was recently named to the Board of Governors of the AIUM. His research interests are in medical imaging, linear and nonlinear acoustics, and digital halftoning.